

Article

Spin-coating of Graphene Oxide as Counter Electrode for Dye-sensitized Solar Cells in Various Dispersing Solvents

Tian-Chiuan Wu, Wei-Ming Huang, Yu-Chi Tsao and Jenn-Kai Tsai *

Department of Electronic Engineering, National Formosa University, Yunlin 632, Taiwan.

* Correspondence: tsajk@nfu.edu.tw

Received: Nov 13, 2022; Accepted: Dec 13, 2022; Published: Dec 30, 2022

Abstract: Platinum (Pt) is the most commonly used counter electrode material for DSSCs. However, as Pt is a noble metal and expensive, researchers have tried to replace the Pt counter electrode with a variety of materials. In this study, graphene oxide (GO) powders were added to solvents of different polarities as precursor solutions for the counter electrode. The solvents were deionized water, dimethylformamide, isopropanol, and chlorobenzene in descending order of polarity. The prepared GO precursor solutions were coated on the Fluorine doped Tin Oxide (FTO) glass substrate via spin coating, then coated substrate subjected to thermal reduction reaction to obtain reduced graphene oxide, which was used as the counter electrode of the DSSC. The photoelectric conversion efficiency (PCE) of DSSC using deionized water as the dispersing solvent was 2.70%, which was five times higher than that of DSSC using chlorobenzene.

Keywords: DSSC, Spin-coat, Graphene oxide, Counter electrode, Dispersion solvents

1. Introduction

The research on solar cells focuses on converting solar energy into electrical energy by using the photovoltaic effect and is divided into crystalline material solar cells, thin film solar cells, organic and polymer cells, hybrid solar cells, and dye-sensitized solar cells (DSSC) depending on raw materials used [1]. Recently, silicon solar cell is the most common and available in the market. Its manufacturing process is similar to a semiconductor, which allows excellent photoelectric conversion efficiency, fast mass production, and high yield. However, the cost of silicon solar power generation and the energy consumed in the production are still much higher than conventional electricity production, so the development of low-cost and high-efficiency solar cells has become the aim of related research all the time. Among various types of solar cells, DSSC has the advantages of low-cost, simple process, and less process equipment, which meets the expectations of researchers.

The general DSSC structure is shown in Fig. 1. Fluorine-doped Tin Oxide (FTO) glass is used as the substrate as it is transparent and conductive, and TiO_2 nanoparticle was used as photoanode. The porous structure of the photoanode is conducive to adsorbed dye. The prepared TiO_2 photoanode and counter electrode (based on platinum and RGO) were sealed with a thermal shrink film as a spacer, and then the electrolyte was filled to complete the DSSC device. The working principle of DSSC consists of four basic steps: light absorption, electron injection, transport carrier, and current collection [2].

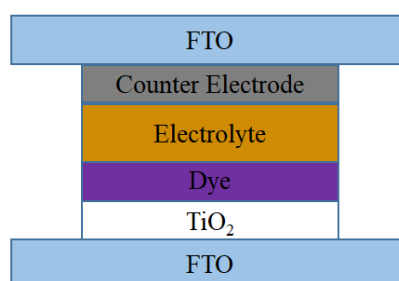


Fig. 1. Schematic diagram of the basic structure of DSSC.

The role of the counter electrode in the DSSC is to accept and transfer electrons into the electrolyte. Thus, it is important to have an efficient catalyst. As a counter electrode, Pt is the most commonly used. In order to reduce the use of noble metals and the

cost of fabricating DSSCs, researchers have tried to replace noble metals to manufacture counter electrodes with various materials such as carbon, alloys, conducting polymers, and other composite materials [3]. The two-dimensional nature of graphene allows for faster conduction to charge than other materials. Its unique honeycomb structure provides excellent electrical conductivity and low resistivity for DSSC applications. Graphene also has been used in fabricating DSSC because of its excellent electrical, optical, and mechanical properties. Graphene was first used to replace FTO in working electrodes in 2008 and has been used to improve TiO₂ layers and its electrolyte transport. Recently, it is replacing Pt [4]. Reducing graphene oxide is the most promising method for the mass production of graphene. Graphene oxide is exfoliated in water by various methods, such as sonication, strong oxidants, or intercalation compounds, resulting in stable graphene oxide suspensions [5–7]. Graphene oxide is obtained by chemical, electrochemical, or thermal reduction, and the resulting material is named reduced graphene oxide (RGO). The structure and properties of graphene are intermediate between graphene oxide and pristine graphene, depending on the degree of reduction and initial structure of graphene oxide [8–10].

This study was carried out to investigate the effect of different solvents for dispersion in graphene oxide solution and preparing the solution into reduced graphene oxide which is used as a counter electrode of DSSC. The graphene oxide solution was coated on the FTO glass substrate by spin coating method to form the graphene oxide on it by simple thermal reduction to form an RGO film. The effects of different dispersion solvents on DSSC were also studied.

2. Materials and Methods

2.1. Materials

The materials used in this study included FTO glass (6 Ω/square), TiO₂ (P25), methanol (CH₃OH, 99%), ethanol (C₂H₅OH, 95%), acetone (CH₃COCH₃, 99.9%), dimethylformamide (DMF, C₃H₇O, 99.8%), chlorobenzene (CB, C₆H₅Cl, 99.5%), isopropanol (C₃H₈O, 99.9%), tert-butyl alcohol (99.9%), DMPII (98%), iodine (99.9%), 3-methoxypropionitrile (98%), 4-tert-butylpyridine (tBP, 99%), N₃ dye, ionomer resin (60 μm), and graphite oxide (GO, C > 45 wt%, O > 45 wt%).

2.2. DSSCs Preparation

2.2.1. Preparation of Substrate

First, two pieces of FTO glass (1.5 cm × 3.0 cm) were prepared and used as the counter electrode which was drilled to make a hole. Second, the FTO glass was cleaned with alcohol to remove dust and glass fragments from its surface. Third, the glass was immersed in acetone, methanol, and deionized water successively and was treated with ultrasonic for 5 min. Finally, the glass was taken out and dried with a nitrogen duster gun and in an oven to dry the residual water.

2.2.2. Preparation of Working Electrode

Working electrodes in this study were prepared according to the following process. First, 10 wt% TiO₂ paste was prepared to contain TiO₂ nanoparticles, tert-butanol, and deionized water which were mixed in a ratio of 1.7078 g, 12 ml, and 6 ml, respectively. Then, the TiO₂ paste was stirred at 300 RPM for at least 12 h. The TiO₂ paste was coated on the FTO glass by the doctor blade method and pressurized with a hydraulic press machine after the film was completely dried. Finally, the coated FTO glass was annealed at 150 °C for 1.5 h, then stayed at 450 °C for 0.5 hours, and finally soaked in N₃ dye for at least 4 h to complete the preparation.

2.2.3. Preparation of Counter Electrode

First, 1 wt% GO solutions using different dispersion solvents (deionized water, DMF, isopropanol, and chlorobenzene) were prepared. Then, the GO solution was coated on the FTO substrate via spin-coating, then heated to 90 °C to evaporate the dispersion solution, and then the coated FTO substrate was heated under 450 °C for 15 min to complete the preparation.

2.2.4. DSSC Assemble

First, the photoanode and counter electrode were sealed together. Secondly, an electrolyte was injected into the hole of the counter electrode. Then, the hole was sealed with glass, and silver conductive epoxy adhesive was applied on the photoanode and the counter electrode to complete the DSSC assemble.

3. Results and Discussions

Fig. 2 shows shaken GO solutions using different dispersion solvents of deionized water (DI), DMF, isopropanol, and chlorobenzene. The GO solution with DI water clung to the bottle and was thicker than other solutions. The GO solution in DMF showed uniformity, which implied better film morphology and thickness as a counter electrode of DSSC. However, the GO solutions in isopropanol and chlorobenzene were less homogeneous than the other two solutions.

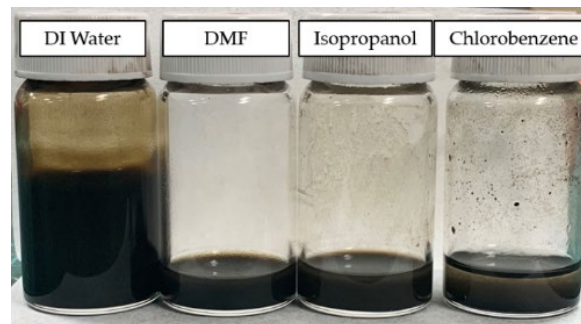


Fig. 2. GO solution in different solvents such as deionized water, DMF, isopropanol, and chlorobenzene.

The DSSC measurement data using different parameters in Tables 1–3 showed that the DSSCs fabricated with 1.00 wt% GO content, a spin coating speed of 2000 RPM, and a thermal reduction temperature of 450 °C had the highest photoelectric conversion efficiency. Therefore, these three process parameters were chosen for the follow-up process.

Table 1. J-V characteristics of DSSC using different GO contents.

GO Content (wt%)	V _{oc} (V)	J _{sc} (mA/cm ²)	F.F. (%)	η (%)
0.25	0.75	8.646	18.201	1.18
0.50	0.72	8.608	24.079	1.50
0.75	0.74	9.187	24.912	1.70
1.00	0.71	7.644	33.314	1.81
1.50	0.72	6.745	29.040	1.41

Table 2. J-V characteristics of DSSC using different spin coating speeds.

Rotating Speed (rpm)	V _{oc} (V)	J _{sc} (mA/cm ²)	F.F. (%)	η (%)
1000	0.72	12.239	14.289	1.25
2000	0.72	11.575	17.737	1.48
3000	0.72	11.768	14.891	1.26

Table 3. J-V characteristics of DSSC using different reduction temperatures.

Thermal Reduction Temperature (°C)	V _{oc} (V)	J _{sc} (mA/cm ²)	F.F. (%)	η (%)
400	0.62	8.557	25.976	1.36
425	0.55	8.412	29.506	1.37
450	0.71	8.696	29.774	1.83
475	0.65	9.429	25.723	1.58
500	0.70	8.079	23.406	1.33

Fig. 3(a–d) shows the real images and Fig. 3(e–h) presents the SEM images of RGO films fabricated using different dispersion solvents. The RGO in DI water as a dispersion solvent had the most uniform morphology, while that in DMF and isopropanol had high transparency but uncertain uniformity. The RGO in chlorobenzene had small particles in it, which means that the RGO formed agglomeration (Fig. 3(a–d)). The SEM images reveal that the RGO film in DI water as a dispersion solvent had the most uniform morphology, while the RGO film in isopropanol and chlorobenzene had a few agglomerations (Fig. 3(e–h)). The RGO film in chlorobenzene formed an accumulation of agglomerations.

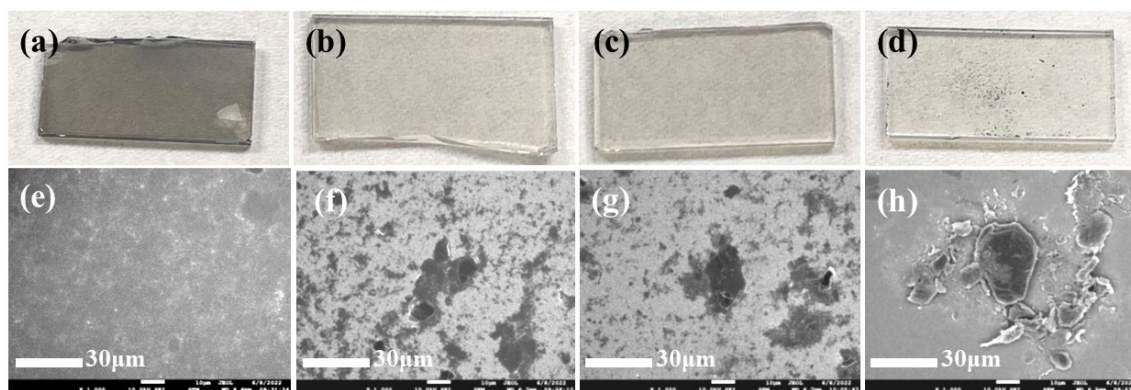


Fig. 3. (a–d) are the real scale photographs and (e–h) are SEM images of RGO films based on (a), (e) DI water; (b), (f) DMF; (c), (g) isopropanol; (d), (h) chlorobenzene as dispersion solvent, respectively.

In order to observe the agglomeration of the RGO films better, X-ray energy dispersive spectroscopy (XEDS) was used to confirm the composition of the films (blue represents carbon). Fig. 4 shows that when the polarity decreased, the agglomerated particles became larger, which impacted the surface area of the RGO film.

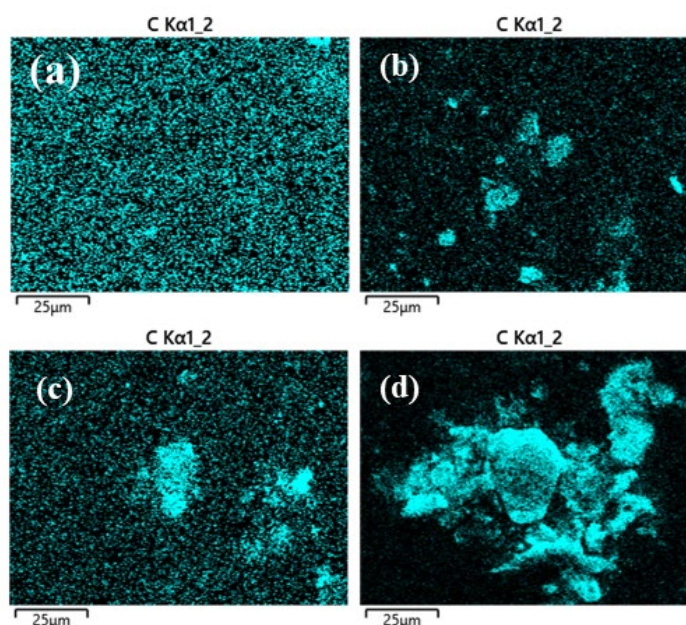


Fig. 4. SEM images of RGO films based on (a) DI water, (b) DMF, (c) isopropanol and (d) chlorobenzene as dispersion solvent, respectively.

The properties of each solvent are described in Table 4 [11]. The polarity of DI water is the highest, followed by DMF, isopropanol, and chlorobenzene. According to the above results, the RGO film formed by the solution with higher polarity has better morphology than the solution with lower polarity.

Table 4. Dielectric constant of DI water, DMF, isopropanol, and chlorobenzene.

Solvent	Dielectric Constant
Deionized water	78.3
DMF	38.3
Isopropanol	20.2
Chlorobenzene	5.62

The RGO film formed by GO raw material in DI water as a dispersion solvent was photographed by transmission electron microscope (TEM) to observe its structure. Although the thermally reduced RGO film structure was transformed into a more ordered and grainier one, the RGO fabricated in this study was heavily oxidized (Fig. 5) [10]. The structure was still different from the expected graphene hexagonal honeycomb structure. The reduction effect of the RGO film prepared at a thermal reduction temperature of 450°C was not as expected. Therefore, the photoelectric conversion efficiency of DSSC made of GO and RGO was validated, and the photoelectric conversion efficiency was used to infer whether its catalytic effect was effective.

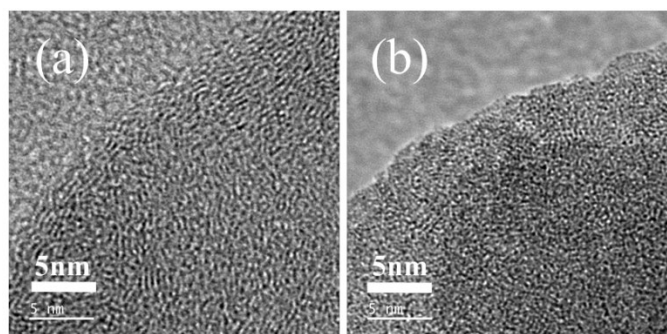


Fig. 5. TEM images of (a) GO raw material and (b) RGO.

The results in Fig. 6 and Table 5 present that although the thermally reduced film was not transformed into the expected graphene hexagonal honeycomb structure, the photoelectric conversion efficiency after encapsulating the GO and RGO counter electrodes into DSSC was significantly different. The photoelectric conversion efficiency of DSSC fabricated with GO counter electrode was almost zero, while the photoelectric conversion efficiency of DSSC fabricated with thermally reduced RGO counter electrode reached 2.70%. This allowed better catalytic activity and electrical conductivity of RGO than those of GO, which effectively improved J_{SC} and photoelectric conversion efficiency.

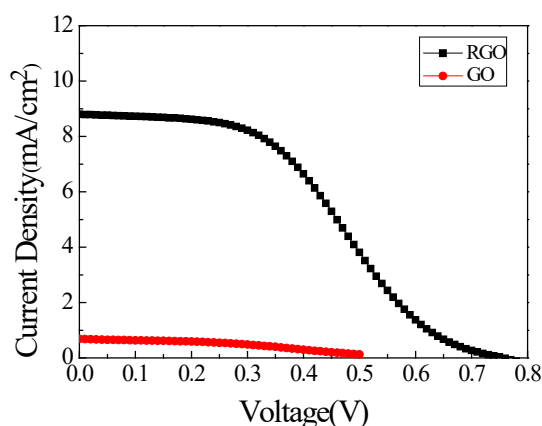


Fig. 6. J-V curves of DSSC based on GO/RGO counter electrodes before and after thermal reduction.

Table 5. J-V characteristics of DSSC using GO/RGO counter electrodes before and after thermal reduction.

	$V_{oc}(V)$	$J_{SC} (mA/cm^2)$	F.F. (%)	η (%)
RGO	0.74	10.001	36.275	2.70
GO	0.50	0.684	43.000	0.0001

Fig. 7 and Table 6 show the EIS measurement results after using different dispersion solvents to make the counter electrode and encapsulate it into DSSC.

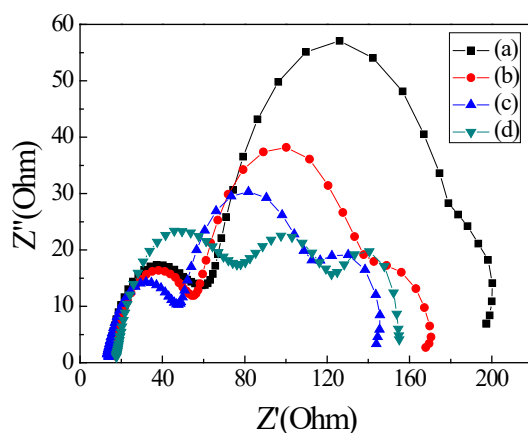


Fig. 7. Nyquist plots of DSSC based on (a) DI water, (b) DMF, (c) isopropanol and (d) chlorobenzene as dispersion solvent, respectively.

Table 6. Electrochemical impedance characteristics of DSSC using RGO counter electrodes before and after thermal reduction.

Dispersing Solvent	R_s (Ω)	R_{GO} (Ω)	R_K (Ω)	R_D (Ω)	K_{eff} (s^{-1})	τ_{eff} (ms)
Deionized water	14.3	44.7	115.4	22.6	37.24	26.8
DMF	16.9	38.4	82.34	30.2	37.24	26.8
Isopropanol	13.8	33.9	68.81	27.2	37.24	26.8
Chlorobenzene	17.6	58.5	45.90	32.9	4152.7	0.24

The R_s , R_{GO} , R_K , K_{eff} , R_D , and τ_{eff} stand for series resistance of wires and bulk, the resistance of charge transit at counter electrode/electrolyte interface, the resistance of electron-hole recombination, the resistance of ion diffusion in the electrolyte, the effective rate constant for recombination of the electron and electron lifetime, respectively [12,13].

Table 6 depicts that although the R_{GO} value of the counter electrode based on DI water had the second highest among the four solutions, while R_K value was the highest (115.4 Ω) and R_D was the lowest (22.6 Ω). This result implied that the counter electrode based on DI water had the most uniform film which improved charge transit. According to the above results, it is inferred that the counter electrode of DSSC made of DI water had the highest efficiency.

Among the dispersing solvents, DI water had the highest R_{GO} value of 44.78 Ω , while isopropanol had the lowest R_{GO} value of 33.93 Ω . Such a difference may be related to the total surface area of the RGO film as shown in Figs. 3 and 4. When the surface area increases, the R_{GO} value decreases, and the agglomerated particles become larger when the polarity is reduced. When using DI water as a dispersing solvent, there is no more increase in surface area. Dispersion becomes uneven owing to agglomeration caused by reduced polarity when using DMF or isopropanol as the dispersing solvent. Therefore, the R_{GO} values of these three polar dispersing solvents were inversely proportional to polarity magnitude.

Fig. 8 and Table 7 show the photoelectric conversion efficiency of DSSC made with different dispersion solvents. The fill factor (F.F.) and photoelectric conversion efficiency showed the same trend as the polarity of the dispersion solvent. The F.F. and photoelectric conversion efficiency of DSSC based on DI water showed the highest polarity as 36.275% and 2.70%, respectively. Those based on chlorobenzene had the lowest polarity as 11.354% and 0.44%, respectively.

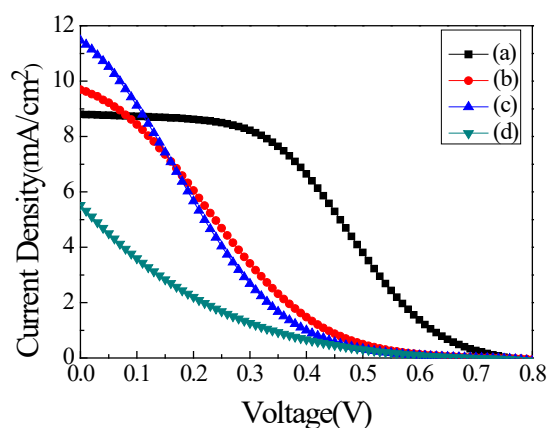


Fig. 8. J-V curves of DSSC based on RGO counter electrodes using (a) DI water, (b) DMF, (c) isopropanol, and (d) chlorobenzene as dispersion solvents.

Table 7. J-V characteristics of DSSC based on RGO counter electrodes using different dispersion solvents.

Dispersing Solvent	V _{oc} (V)	J _{sc} (mA/cm ²)	F.F. (%)	η (%)
Deionized water	0.74	10.001	36.275	2.70
DMF	0.74	9.690	16.924	1.21
Isopropanol	0.72	11.470	13.810	1.15
Chlorobenzene	0.70	5.524	11.354	0.44

4. Conclusions

The photoelectric conversion efficiency can be effectively enhanced by changing the polarity of the dispersion solvent in the counter-electrode precursor solution. The photoelectric conversion efficiency of DSSC based on DI water as a dispersing solvent was 2.70%, which was 513% higher than that of DSSC based on chlorobenzene as dispersing solvent, which is 0.44%. However, such a high improvement in the photoelectric conversion efficiency was attributed to the polarity of the dispersing solvent, which caused the agglomeration of the RGO films to varying degrees. The smaller the polarity of the dispersing solvent, the larger agglomerated crystals and the difference in the surface area of the film. The polarity of DI water was the largest compared to other dispersing solvents. Therefore, using DI water as the dispersion solvent had the best coating result and the highest surface area, resulting in a slower decrease in short-circuit current compared with other dispersion solvents, so DI water allowed the highest photoelectric conversion efficiency.

Author Contributions: J.K. Tsai designed the work and editing the manuscript. T.C. Wu helped in carrying out the FE-SEM and TEM measurement and analysis. W.M. Huang and Y.C. Tsao carried out the preparation of samples, UV-vis absorption, EIS, and J-V measurements. All authors read and approved the final manuscript.

Funding: This research did not receive external funding.

Acknowledgments: The authors would like to thank Hsun-Lin Chan, Li-Jung Liu, Tang-Kai Chen, and Meng-Xiu Chen for their assistance.

Conflicts of Interest: The authors declare no conflict of interest.

References

1. Tyagi, V.V.; Rahim, N.A.A.; Rahim, N.A.; Selvaraj, J.A.L. Progress in solar PV technology: Research and achievement. *Renewable and Sustainable Energy Reviews* **2013**, *20*, 443–461. <https://doi.org/10.1016/j.rser.2012.09.028>
2. Sharma, K.; Sharma, V.; Sharma, S.S. Dye-Sensitized Solar Cells: Fundamentals and Current Status. *Nanoscale Research Letters* **2018**, *13*(1), 381. <https://doi.org/10.1186/s11671-018-2760-6>
3. Chen, M.; Shao, L.-L. Review on the recent progress of carbon counter electrodes for dye-sensitized solar cells. *Chemical Engineering Journal* **2006**, *304*, 629–645. <https://doi.org/10.1016/j.cej.2016.07.001>
4. Park, S.; Ruoff, R.S. Chemical methods for the production of graphenes. *Nature Nanotechnology* **2009**, *4*(4), 217–224. <https://doi.org/10.1038/nnano.2009.58>

5. Brodie, B.C., XIII. On the atomic weight of graphite. *Philosophical Transactions of the Royal Society of London* **1997**, *149*, 249–259. <https://doi.org/10.1098/rstl.1859.0013>
6. Schniepp, H.C.; Li, J.-L.; McAllister, M.J.; Sai, H.; Herrera-Alonso, M.; Adamson, D.H.; Prud'homme, R.K.; Car, R.; Saville, D.A.; Aksay, I.A. Functionalized Single Graphene Sheets Derived from Splitting Graphite Oxide. *The Journal of Physical Chemistry B* **2006**, *110*(17), 8535–8539. <https://doi.org/10.1021/jp060936f>
7. Hwa, T.; Kokufuta, E.; Tanaka, T. Conformation of graphite oxide membranes in solution. *Physical Review A* **1991**, *44*(4), R2235–R2238. <https://doi.org/10.1103/PhysRevA.44.R2235>
8. Gao, W.; Alemany, L.B.; Ci, L.; Ajayan, P.M. New insights into the structure and reduction of graphite oxide. *Nature Chemistry* **2009**, *1*(5), 403–408. <https://doi.org/10.1038/nchem.281>
9. Erickson, K.; Erni, R.; Lee, Z.; Alem, N.; Gannett, W.; Zettl, A. Determination of the Local Chemical Structure of Graphene Oxide and Reduced Graphene Oxide. *Advanced Materials* **2010**, *22*(40), 4467–4472. <https://doi.org/10.1002/adma.201000732>
10. Punckt, C.; Muckel, F.; Wepfer, S.; Aksay, I.; Chavarin, C.; Bacher, G.; Mertin, W. The effect of degree of reduction on the electrical properties of functionalized graphene sheets. *Applied Physics Letters* **2013**, *102*, 023114. <https://doi.org/10.1063/1.4775582>
11. Uversky, V.N.; Narizhneva, N.V.; Kirschstein, S.O.; Winter, S.; Löber, G. Conformational transitions provoked by organic solvents in β -lactoglobulin: can a molten globule like intermediate be induced by the decrease in dielectric constant? *Folding and Design* **1997**, *2*(3), 163–172. [https://doi.org/10.1016/S1359-0278\(97\)00023-0](https://doi.org/10.1016/S1359-0278(97)00023-0)
12. Ali, A.K.; Eli, S.E.; Hassoon, K.I.; Ela, C.; Ahmed, D.S. Design of high-efficiency tandem dye-sensitized solar cell with two-photoanodes toward the broader light harvesting. *Digest Journal of Nanomaterials and Biostructures* **2018**, *13*, 299–305.
13. Omar, A.; Abdullah, H. Electron transport analysis in zinc oxide-based dye-sensitized solar cells: A review. *Renewable and Sustainable Energy Reviews* **2014**, *31*, 149–157. <https://doi.org/10.1016/j.rser.2013.11.031>

Publisher's Note: IIKII stays neutral with regard to jurisdictional claims in published maps and institutional affiliations.

Copyright: © 2022 The Author(s). Published with license by IIKII, Singapore. This is an Open Access article distributed under the terms of the [Creative Commons Attribution License \(CC BY\)](https://creativecommons.org/licenses/by/4.0/), which permits unrestricted use, distribution, and reproduction in any medium, provided the original author and source are credited.